Cell, Vol. 77, 461–472, May 6, 1994, Copyright © 1994 by Cell Press

Nuclear Magnetic Resonance Structure of an SH2 Domain of Phospholipase C-γ1 Complexed with a High Affinity Binding Peptide

Steven M. Pascal,*†§ Alex U. Singer,*†‡ Gerry Gish,‡ Toshio Yamazaki,§ Steven E. Shoelson,‖ Tony Pawson,‡ Lewis E. Kay,§ and Julie D. Forman-Kay*

*Biochemistry Research Division
Hospital for Sick Children
555 University Avenue
Toronto, Ontario M5G 1X8
Canada

‡Division of Molecular and Developmental Biology
Samuel Lunenfeld Research Institute
Mount Sinai Hospital
600 University Avenue
Toronto, Ontario M5G 1X5
Canada

§Protein Engineering Network Centres of Excellence and Departments of Medical Genetics, Biochemistry, and Chemistry
University of Toronto
Toronto, Ontario M5S 1A8
Canada

‖Joslin Diabetes Center
and Department of Medicine
Brigham and Women's Hospital
and Harvard Medical School
Boston, Massachusetts 02215

Summary

The solution structure of the C-terminal SH2 domain of phospholipase C-γ1 (PLC-γ1), in complex with a phosphopeptide corresponding to its Tyr-1021 high affinity binding site on the platelet-derived growth factor receptor, has been determined by nuclear magnetic resonance spectroscopy. The topology of the SH2-phosphopeptide complex is similar to previously reported Src and Lck SH2 complexes. However, the binding site for residues C-terminal to the phosphotyrosine (pTyr) is an extended groove that contacts peptide residues at the +1 to +6 positions relative to the pTyr. This striking difference from Src and Lck reflects the fact that the PLC-γ1 complex involves binding of a phosphopeptide with predominantly hydrophobic residues C-terminal to the pTyr and therefore serves as a prototype for a second class of SH2-phosphopeptide interactions.

Introduction

Src homology 2 (SH2) domains play a vital role in signal transduction processes by binding to sites of Tyr phosphorylation following growth factor stimulation (reviewed by Koch et al., 1991; Cantley et al., 1991; Pawson and Gish, 1992). These modular regions of ~100 residues are found in a number of proteins that act downstream of growth factor receptors (Anderson et al., 1990; Moran et al., 1990). SH2 domain–containing proteins can be roughly subdivided into two groups, those containing an enzymatic activity necessary for downstream signal transduction events, such as members of the Src-related family of cytoplasmic Tyr kinases, Ras GTPase-activating protein and phospholipase C-γ (PLC-γ), and those molecules that have no enzymatic activity and act as so-called adaptor molecules in bridging protein–protein interactions, such as the p85 subunit of phosphoinositol 3-kinase (PI3K), Crk, and members of the Sem-5/Grb2/drk family (Pawson et al., 1993). The tertiary structures of isolated SH2 domains from Abl (Overduin et al., 1992a, 1992b), Src (Waksman et al., 1993), and the p85 subunit of PI3K (Booker et al., 1992) have been determined. These structural studies by nuclear magnetic resonance (NMR) and X-ray crystallographic techniques reveal a similar overall topology for the SH2 domain consisting of a large central β sheet and an associated smaller β sheet, flanked by two α helices. Crystal structures of Src (Waksman et al., 1993) and Lck (Eck et al., 1993) SH2 domains complexed with high affinity binding phosphopeptides representing residues of potential target-binding proteins and containing the sequence pTyr–Glu–Glu–Ile are also available, as are structures of the Src SH2 domain complexed with low affinity binding phosphopeptides (Waksman et al., 1992). These structures reveal a binding mechanism best described as a two-pronged plug. The pTyr inserts into the larger pocket and the Ile at the +3 position relative to the pTyr binds to the smaller pocket. The binding site for the pTyr involves a network of charge–charge and hydrogen bonding interactions between residues of the SH2 domain and the phosphate oxygens and aromatic π electrons of the pTyr ring.

It is expected that the mode of binding of pTyr will be generally conserved for SH2 domains, based on the strong conservation of SH2 residues involved in the SH2–pTyr interaction (Koch et al., 1991). In vitro and in vivo studies (reviewed by Cantley et al., 1991; Pawson and Schlessinger, 1993) have shown that sequence-specific high affinity binding between an SH2 domain and its target depends on amino acids flanking the pTyr residue. Relative binding affinities of phosphopeptides generated from libraries in which the three residues immediately C-terminal to the pTyr have been randomized support the hypothesis that these residues confer the primary specificity of SH2 interaction (Songyang et al., 1993, 1994). Based on these specificities and the identity of a particular (βD5) amino acid in the SH2 domain, Cantley and coworkers divided SH2 domains into two categories (Songyang et al., 1994), those that bind sequences with the motif pTyr–hydrophilic–hydrophilic–Ile/Pro and those that bind sequences with the motif pTyr–hydrophobic–X–hydrophobic. Members of the first class include SH2 domains of nonreceptor

†The first two authors contributed equally to this work.

Tyr kinases. Members of the second class include the SH2 domains of the p85 subunit of PI3K, SH2-containing pTyr phosphatases, and PLC-γ.

PLC performs the enzymatic hydrolysis of inositol-containing phospholipids, releasing the second messengers inositol triphosphate and diacylglycerol. The γ isoforms of PLC are regulated by growth factor stimulation owing to the presence of their two SH2 domains, which other isoforms lack (Rhee, 1991). PLC-γ SH2 domains bind to specific sites of phosphorylation in the platelet-derived growth factor receptor (PDGFR) (Valius et al., 1993; Valius and Kazlauskas, 1993), epidermal growth factor receptor (EGFR) (Rotin et al., 1992; Zhu et al., 1992) and Flg fibroblast growth factor receptor (FGFR) (Mohammadi et al., 1991). Mutation of Tyr-1021 of the PDGFR to Phe blocks in vivo PLC-γ binding and phosphoinositide hydrolysis following PDGF stimulation (Valius et al., 1993). The K_D value for the interaction of the C-terminal SH2 domain of PLC-γ (PLCC) with a 12 residue phosphopeptide having a sequence derived from this Tyr-1021 site (pY1021 peptide) is $\sim 1 \times 10^{-7}$ to 5×10^{-7} M, estimated by competition assay (Piccione et al., 1993) and calorimetry (S. E. S., unpublished data). These estimates are consistent with determinations of the concentration of the pY1021 peptide necessary to inhibit 50% of the binding of intact PLC-γ to the C-terminal tail of the PDGFR (Larose et al., 1993).

While a number of SH2-containing proteins bind to activated PDGFR both in vivo and in vitro, recent studies demonstrate that interactions with PLC-γ are biologically significant for the mitogenic effects of PDGF. In vivo binding studies with PDGFR mutations of Tyr to Phe indicated that either Tyr-751 (the target for the SH2 domains of the p85 subunit of PI3K and Nck) or Tyr-1021 (the target for the PLC-γ SH2) was necessary for Ras activation and transmission of a mitogenic signal (Valius and Kazlauskas, 1993). In a previous study, mutation of Tyr-1021 was shown to decrease the PDGF mitogenic response by ~30% (Valius et al., 1993). Interactions of PLC-γ with other receptors seem to be less important for their mitogenic response (Peters et al., 1992; Mohammadi et al., 1992). Thus, the high affinity binding of PLC-γ to Tyr-1021 of the PDGFR is a significant biological interaction in signaling processes.

While both SH2 domains of PLC-γ belong to the category of those that bind pTyr–hydrophobic–X–hydrophobic sequences, the N- and C-terminal SH2 domains of PLC-γ1 have different sequence specificities. Binding studies with randomized peptides (Songyang et al., 1993) show that the N-terminal domain prefers an acidic residue at the +2 position relative to the pTyr while the C-terminal SH2 domain prefers a hydrophobic amino acid at this position. The sequences of the Tyr-1021 PLC-γ1 site of the PDGFR and the Tyr-992 site of the EGFR, pTyr–Ile–Ile–Pro and pTyr–Leu–Ile–Pro, respectively, match the specificity of the C-terminal SH2, while the sequence of the Tyr-766 site of the FGFR, pTyr–Leu–Asp–Leu, matches the specificity of the N-terminal SH2 of PLC-γ. Thus, the biological interaction of PLC-γ with Tyr-1021 of the PDGFR is most likely due to the C-terminal SH2 domain of the enzyme. Therefore, we have studied the complex of the C-terminal SH2 of PLC-γ1 with a phosphopeptide encompassing the Tyr-1021 of the PDGFR.

Comparison of structures of several SH2 domain–target peptide complexes should help to deepen our understanding of the molecular details of sequence-specific protein interactions in signal transduction. The crystal structures of the Src SH2 domain (Waksman et al., 1993) and the highly homologous Lck SH2 domain (Eck et al., 1993) complexed with a high affinity binding phosphopeptide containing the sequence pTyr–Glu–Glu–Ile are representative of the specific binding of pTyr–hydrophilic–hydrophilic–Ile/Pro sequences to SH2 domains. In this paper, we present the solution structure of the complex of the C-terminal SH2 domain of PLC-γ1 with a phosphopeptide corresponding to its high affinity Tyr-1021-binding site in PDGFR β. The sequence of this 12 residue pY1021 peptide, Asp–Asn–Asp–pTyr–Ile–Ile–Pro–Leu–Pro–Asp–Pro–Lys, contains the pTyr–hydrophobic–X–hydrophobic motif. Thus, this structure provides an example of complexes representative of the second category of SH2–pTyr peptide interactions as well as the structure of a known biologically relevant SH2 interaction, since the biological targets of the Src and Lck SH2 domains are not as well characterized as those of the C-terminal SH2 of PLC-γ.

Results

NMR Analysis of the SH2-pY1021 Complex

Uniform ^{13}C and ^{15}N labeling of proteins can facilitate NMR studies of their interactions with unlabeled target ligands (Ikura and Bax, 1992). The C-terminal SH2 domain of bo-

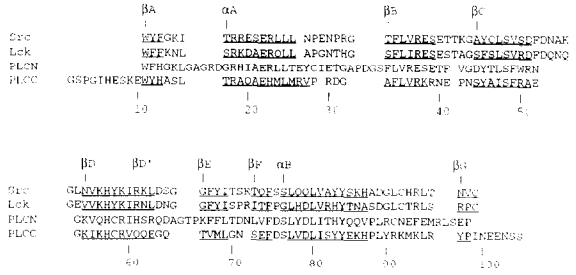

Figure 1. Sequence Alignment of the PLCC SH2 Domain with the Src and Lck SH2 Domains Based on a Comparison of the PLCC and Src SH2 Structures

Owing to the similarity of sequences of the two SH2 domains of PLC-γ1, an alignment of the N-terminal SH2 domain of PLC-γ1 (PLCN) with the other SH2 sequences based on the structure of the PLCC SH2 is also given. The secondary structural elements in the PLCC SH2 domain and those from the Src (Waksman et al., 1993) and Lck (Eck et al., 1993) complexes are underlined. The nomenclature proposed by Harrison and coworkers (Eck et al., 1993) is indicated at the first residues of the secondary structural elements to which they refer. Note that there are differences in this alignment from those published previously, including the definition of strand βF in the PLCC SH2 domain and the alignment for helix αA. While helix αB in the PLCC begins one residue later than the helices in the Src and Lck structures, the residues will be numbered according to the Src/Lck nomenclature. Residue numbers of the PLCC SH2 domain construct used in this study are given below the sequence.

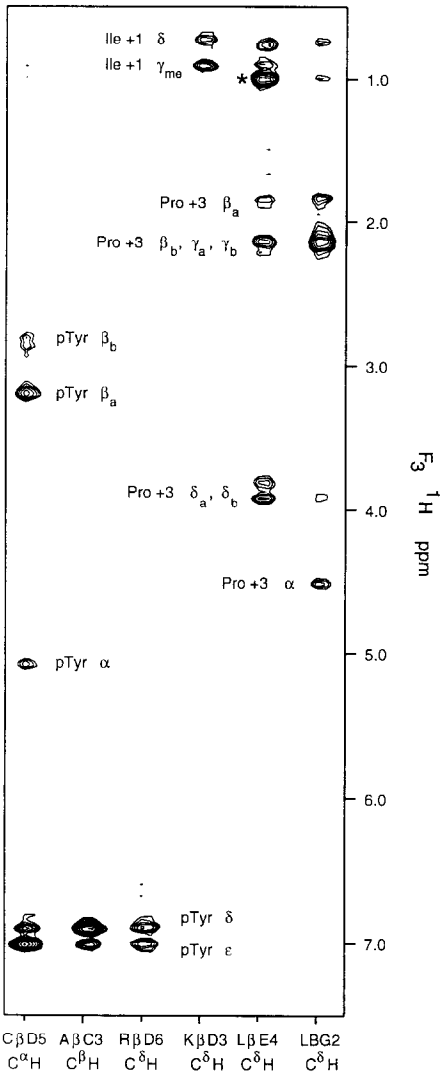

Figure 2. Selected NOE Correlations between the PLCC SH2 Domain and pY1021 Peptide

^{13}C-^{1}H strips taken from a 150 ms mixing time 3D F_1-edited, F_3-filtered NOESY in D_2O at 30°C, showing representative NOE correlations between protons of the PLCC SH2 domain and pY1021 peptide. These include cross peaks from resonances of the pTyr to those of Cys βD5, Ala βC3, and Arg βD6; from resonances of Ile +1 to Lys βD3; and from resonances of Pro +3 to Leu βE4 and Leu BG2. The asterisk indicates an NOE to one or more of the overlapping resonances of the Ile +2 Cγ methyl or the Leu +4 Cδ methyls.

vine PLC-γ1 (PLCC) (Figure 1), comprising residues 663–759 of the full enzyme (Stahl et al., 1988), was expressed from Escherichia coli grown in minimal media with the addition of ^{13}C-glucose and ^{15}N-ammonium chloride to prepare 99% isotopically enriched protein. Yields of 50 mg of PLCC SH2 domain per liter of culture could be obtained. The PLCC SH2 domain was most soluble in phosphate buffers and gave well-dispersed NMR spectra at pH 6.4 and 30°C. The synthetic 12 residue pY1021 phosphopeptide (unlabeled) was titrated into an NMR sample of 1.5 mM free PLCC SH2 in 100 mM phosphate buffer (pH 6.4) until a 1:1 complex of SH2:phosphopeptide was achieved.

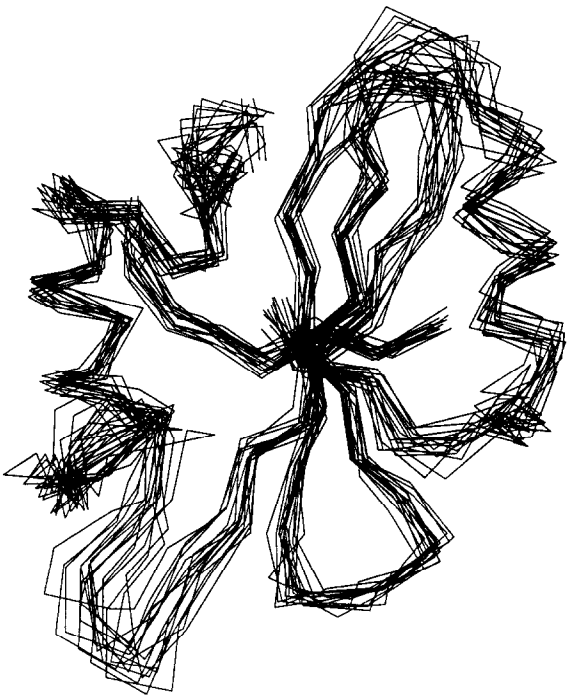

Figure 3. Superposition of the Cα Atoms of the 18 Final Simulated Annealing Structures of the PLCC SH2–pY1021 Complex

Structures were generated using the program X-PLOR (Brünger, 1992). Cα atoms of the central β sheet and two helices of the SH2 domain (residues 11–13, 19–26, 33–39, 44–51, 55–62, and 78–87) were superimposed for this figure. Residues 1–10 and 100–105 of the SH2 domain and the first two and last two residues of the phosphopeptide are disordered in solution and are excluded from the figure.

Titration led to broadening and disappearance of resonances of the uncomplexed PLCC SH2 and a sharpening and increase in intensity of peaks of the SH2–pY1021 complex. The predominantly slow exchange behavior between the two states, free and complexed, is consistent with the high affinity binding of the pY1021 peptide to the PLCC SH2 domain.

NMR experiments exploiting heteronuclear editing and filtering techniques allow specific interactions between two molecules, one ^{13}C and ^{15}N labeled and another unlabeled, to be identified, as well as interactions within each of the two molecules to be studied separately (Ikura and Bax, 1992). Three-dimensional (3D) heteronuclear techniques that allow observation of interactions between protons bound to ^{13}C or ^{15}N atoms were used to determine resonance assignments and the structure of the SH2 domain. Filtered two-dimensional (2D) experiments, which eliminate proton resonances bound to ^{13}C and ^{15}N atoms, were used to determine the assignments and nuclear Overhauser effect (NOE) correlations within the pY1021 peptide. Finally, NOEs between the SH2 and the pY1021 peptide were assigned via half-filtered experiments in which the ^{13}C or ^{15}N and their attached protons are correlated with protons attached to ^{12}C and ^{14}N. Figure 2 shows portions of a 3D half-filtered NOE spectroscopy (NOESY) spectrum demonstrating interactions between protons of

Table 1. Structural Statistics and Atomic RMSDs of the 18 Final Structures of the PLCC SH2–pY1021 Complex

Structural statistics[a]	<SA>	$(SA)_r$
RMSDs from NOE-derived distance restraints (Å)		
All (1239)	0.015 ± 0.001	0.010
SH2–SH2 distances (1104)	0.013 ± 0.001	0.006
pY1021–pY1021 distances (37)	0.025 ± 0.004	0.041
SH2–pY1021 distances (98)	0.019 ± 0.001	0.010
H-bonds (50)[b]	0.022 ± 0.003	0.013
RMSDs from experimental dihedral restraints (degrees) (82)[c]	0.335 ± 0.139	0.165
Deviations from idealized geometry		
Bonds (Å) (1929)	0.0016 ± 0.0002	0.001
Angles (degrees) (3482)	0.582 ± 0.015	0.564
Impropers (degrees) (1016)	0.319 ± 0.031	0.279
Atomic RMSDs (Å)[d]	Backbone	All
Residues 11–99 (89)	1.17 ± 0.18	1.94 ± 0.17
Central β sheet (βA, βB, βC, and βD) (22)	0.52 ± 0.10	1.33 ± 0.14
pTyr-binding site (7)	0.43 ± 0.10	1.43 ± 0.20
Hydrophobic binding groove (16)	0.61 ± 0.51	1.26 ± 0.28
Complete binding interface (23)	0.64 ± 0.17	1.36 ± 0.21

[a] The average RMSDs from the experimental and covalent geometric restraints used for the X-PLOR structure calculations are listed. <SA> represents the mean value for the 18 final simulated annealing structures; $(SA)_r$ is the restrained minimized mean structure, where the mean structure was obtained by averaging the coordinates of the 18 individual superimposed structures. The number of terms for the various restraints is given in parentheses. None of the structures exhibited distance violations greater than 0.3 Å or dihedral angle violations greater than 4°.

[b] For each hydrogen bond there are two restraints: r_{NH-O}, 1.5–2.3 Å; r_{N-O}, 2.4–3.3 Å. A total of 50 restraints were used for 25 constrained H bonds. All hydrogen bond restraints involved slowly exchanging amide protons and were included only if the acceptor could be unambiguously defined by local NOEs.

[c] Torsion angle restraints included 65 ϕ, 7 ψ, and 8 χ^1 angles for the SH2 domain, based on $^3J_{HN\alpha}$ values and NOE-derived intraresidue and sequential distances from 50 ms mixing time NOESY spectra. In addition, 2 χ^1 angles of the peptide were restrained based on intraresidue and sequential NOEs and the results of initial structure calculations.

[d] The average atomic RMSDs from the mean structure for the backbone atoms (including the N, Cα, and C′) of the indicated residues are listed, as well as for all nonhydrogen atoms of those regions, with the number of residues involved given in parentheses. The residues of the pTyr-binding site are Glu αA6, Arg βB7, Ala βC3, His βD4, pCys βD5, Arg βD6, and the pTYr. The residues in the hydrophobic binding groove are Ile βC4, Phe βC6, Lys βD3, Cys βD5, Leu βE4, Gly EF1, Asn EF2, Pro BG1, Leu BG2, Tyr BG3, Arg BG4, Ile +1, Ile +2, Pro +3, Leu +4, and Pro +5.

the PLCC SH2 domain and pY1021 peptide. The 2D and 3D double and triple resonance experiments utilized are described in Experimental Procedures.

3D structures were computed utilizing a combined distance geometry-simulated annealing protocol using the program X-PLOR (Brünger, 1992). The calculations included 1104 protein–protein NOE-derived distance restraints, 65 ϕ and 7 ψ torsion angle restraints, and restraints for 25 hydrogen bonds. A total of 98 NOEs between the PLCC SH2 domain and pY1021 peptide and 37 NOEs within the pY1021 were also included. A superposition of the Cα coordinates from the 18 final X-PLOR structures is shown in Figure 3. The average root mean–squared deviation (RMSD) from the mean structure for ordered backbone atoms, including residues 11–99 of the PLCC SH2 domain, is 1.17 Å (Table 1). The backbone RMSD for the central β sheet, including residues 11–13, 34–38, 44–51, and 54–60, is 0.52 Å. The RMSD for backbone atoms and for all heavy atoms of residues of the SH2 domain and pY1021 peptide in the binding interface, including residues 22, 39, 46, 47, 49, 56–59, 69–71, and 88–91 for the SH2 and the pTyr and the following five residues of the peptide, are 0.64 Å and 1.36 Å, respectively. A superposition of selected side chains of the hydrophobic binding interface from the ensemble of structures is shown in Figure 4, with an RMSD for these atoms of 0.72 Å. This level of precision allows the detailed description of many specific interactions of the SH2 domain with the pY1021 peptide. The structures have no NOE violations greater than 0.3 Å, no torsion angle violations greater than 4°, and very low deviation from ideal covalent geometry.

Overall Topology of the PLCC SH2-Peptide Complex

The topology of the PLCC SH2 is very similar to that of other SH2 domains that have been studied (Overduin et al., 1992a, 1992b; Waksman et al., 1992, 1993; Booker et al., 1992; Eck et al., 1993). Figure 5A is a schematic ribbon diagram of the backbone of the minimized mean structure. The central β sheet is composed of four primary strands, βA, βB, βC, and βD. An additional extended region can be defined as a short β strand, βG from Tyr-97 to Pro-98, based on one hydrogen bond to βB, but the extent of the interaction is minimal. Strand βD continues as βD′, the first strand of the second β sheet. This smaller sheet is composed of three strands, βD′, βE, and βF. The connections between strands βC and βD, strands βD′ and βE, and strands βE and βF are tight β turns. The α helices flank the central sheet, and the C-terminus of the second α helix is slightly irregular, with some bifurcated or missing hydrogen bonds. The N- and C-termini of the PLCC SH2

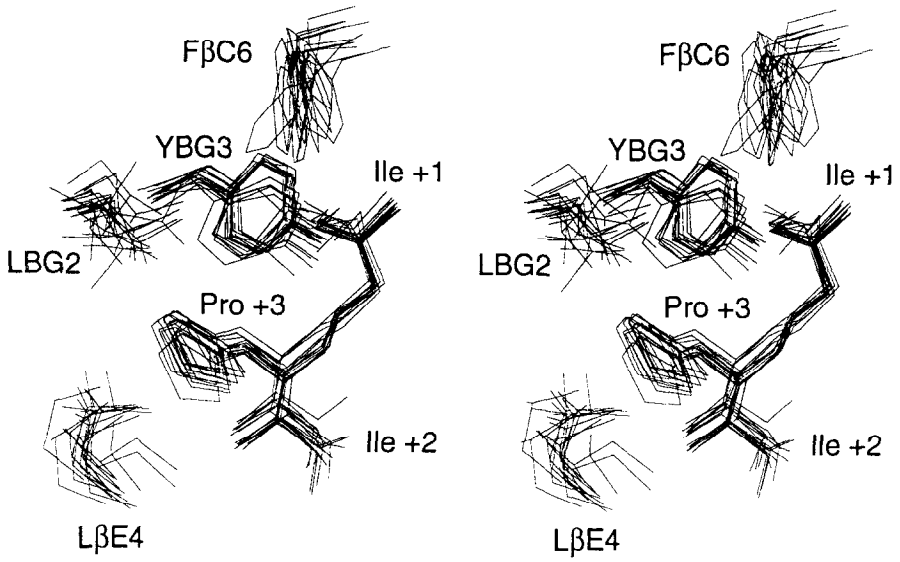

Figure 4. Superposition of Selected Residues of the Hydrophobic Binding Interface

Stereoview from the ensemble of simulated annealing structures of the SH2 PLCC–pY1021 complex with side chain heavy atoms (including the Cα) for residues Phe βC6, Leu βE4, Leu BG2, and Tyr BG3 of the SH2 domain and all heavy atoms for the three residues C-terminal of the pTyr of the peptide (from the Cα of Ile +1 to the Cα of Pro +3).

domain are located on the opposite side of the protein from the peptide binding surface. Loops between strands βE and βF (EF loop) and between helix αB and strand βG (BG loop) are intimately involved in interactions with pY1021 peptide residues C-terminal to the pTyr. The BG loop contains a β-turn structure with a bifurcated hydrogen bond from the amide protons of Leu BG2 and Tyr BG3 to the carbonyl of Met BG6. The binding site of the PLCC SH2 domain can be described as a pocket for the pTyr residue and a long deep groove for residues C-terminal to

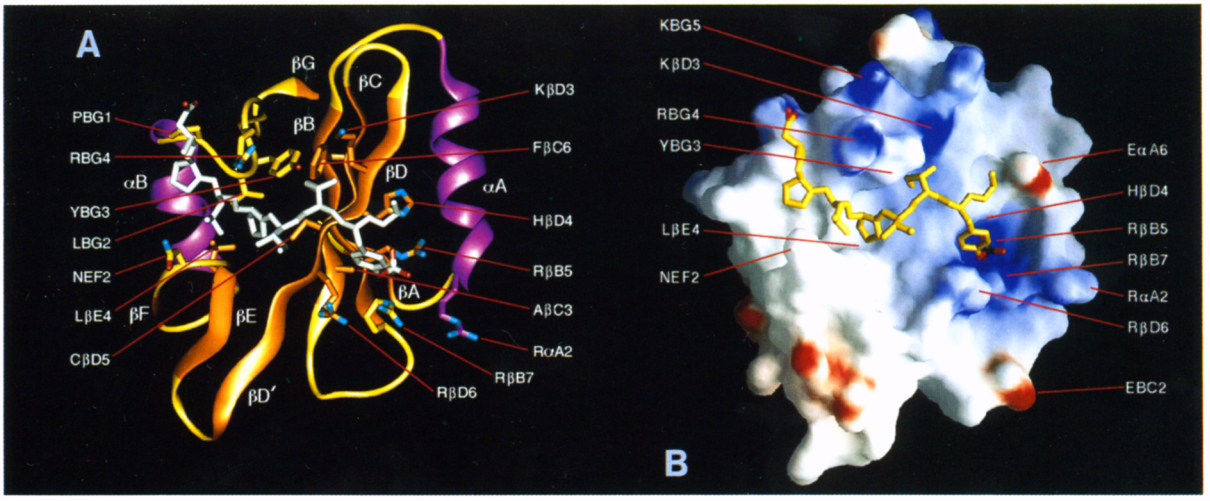

Figure 5. Interactions between the PLCC SH2 Domain and pY1021 Peptide

Important residues are identified with red arrows.

(A) Cartoon drawing. The backbone of the SH2 domain is shown as a ribbon (residues 11–99) with orange β strands (βA, Trp-11 to His-13; βB, Ala-34 to Lys-38; βC, Phe-45 to Ala-51; βD, Lys-54 to Val-60; βD′, Gln-61 to Glu-63; βE, Thr-66 to Leu-69; βF, Ser-72 to Phe-74; and βG, Tyr-97 to Pro-98), violet α helices (αA, Thr-17 to Val-28; αB, Leu-77 to His-87), and yellow turns and loops. Nonhydrogen atoms of peptide residues 4–10 (in white) and SH2 side chains that interact with the peptide.are shown as licorice bonds, with oxygen and nitrogen side chain atoms colored red and blue, respectively. The figure was created by QUANTA Release 3.3 (Molecular Simulations Incorporated, University of York, York, England).

(B) Molecular surface of the PLCC SH2 domain with the identical residues of the pY1021 peptide as in (A) drawn with licorice bonds. Blue represents positive and red negative electric potential calculated using default charges, with the peptide removed, and displayed using the program GRASP (Nicholls et al., 1991). Note the intense positive potential at the bottom of the pTyr-binding pocket, as well as the apolar nature of the large hydrophobic binding groove.

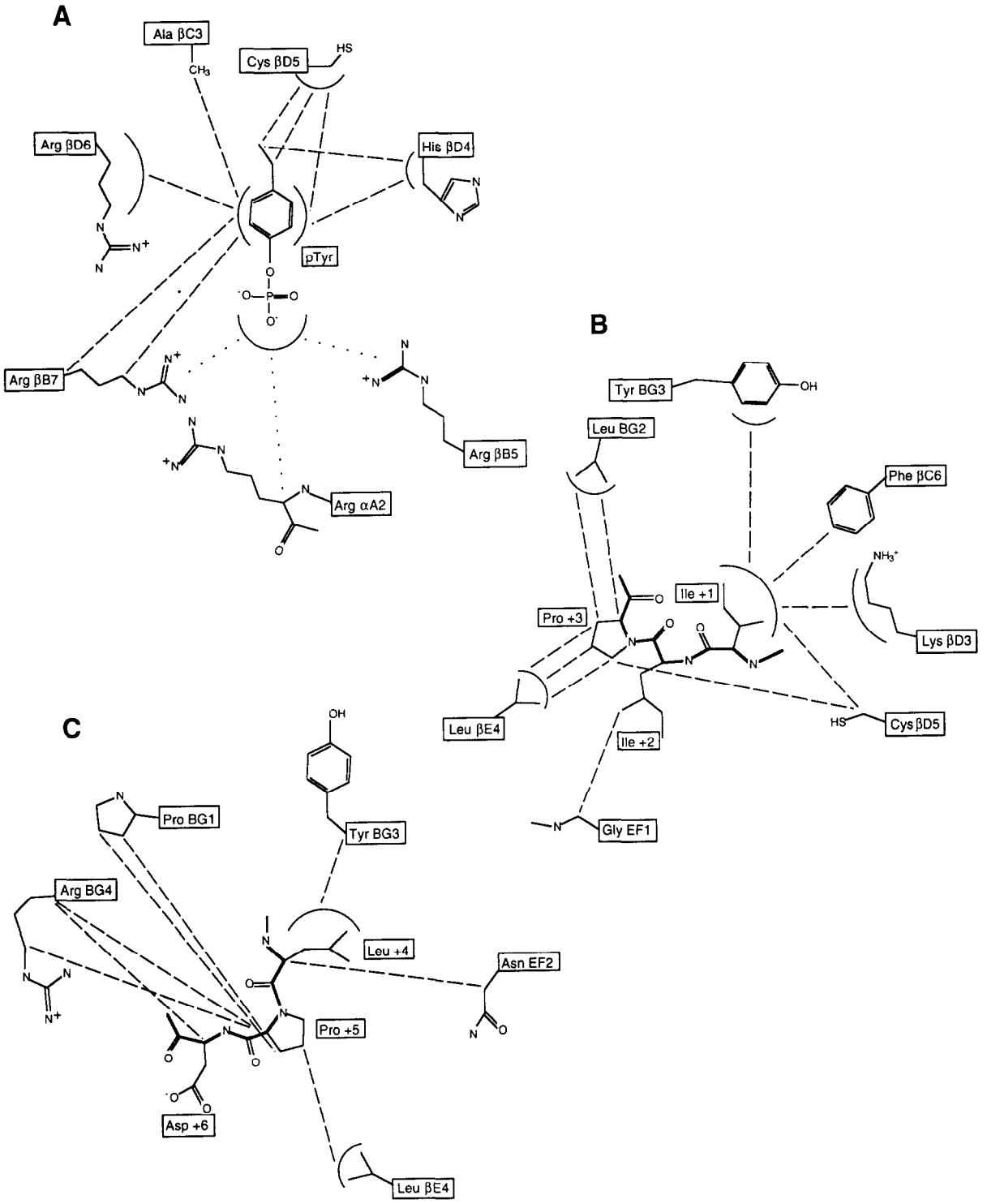

Figure 6. Schematic Illustration of Strong and Medium NOE Correlations between the PLCC SH2 Domain and pY1021 Peptide, Indicating Distances of ~4 Å or Less

The NOEs are represented as dashed lines. For clarity, when multiple NOEs from an amino acid are present, the relevant region of the amino acid is enclosed by an arc and the NOEs are drawn from the arc.

(A) NOEs between the SH2 domain and pTyr. Structures in which the guanidinium groups of Arg βB5 and Arg βB7 are within hydrogen bonding distance of the phosphate group of the pTyr are present in the calculated ensemble. Although no NOEs to guanidinium protons were observed from these residues and from Arg αA2, other evidence suggests the presence of these contacts (see text), which are indicated as dotted lines. Structures in which the guanidinium group of Arg βD6 is within hydrogen bonding distance of the π electron cloud of the pTyr are also present in the calculated ensemble.

(B) NOEs between the SH2 domain and Ile +1, Ile +2, and Pro +3 of the pY1021 peptide.

(C) NOEs between the SH2 domain and Leu +4, Pro +5, and Asp +6 of the pY1021 peptide.

the pTyr, accommodating residues at positions +1 through +6 relative to the pTyr. This binding cavity is orthogonal to the central β sheet with borders defined by strand βD, the EF loop, and the BG loop. Although there are slight differences in the exact positions of the secondary structural elements of this PLCC SH2 structure from those of the Src and Lck SH2 domains described by Eck et al. (1993) and Waksman et al. (1993), the nomenclature initiated in those papers that relates amino acids to secondary structural elements will be utilized (see Figure 1).

pTyr-Binding Site

Important contacts between the PLCC SH2 domain and pY1021 peptide are shown in Figure 5A. The pTyr interacts with a positively charged region of the protein including residues Arg αA2, Arg βB5, Arg βB7, and Arg βD6. (Note that His βD4 is neutral, based on chemical shift data.) As can be seen in the electrostatic surface of the PLCC SH2 domain shown in Figure 5B, this concentration of positive charges creates an intense positive field at the bottom of the phosphate-binding pocket formed by residues in helix αA and strands βB, βC, and βD (Figure 5A). Figure 6A shows schematically the NOE contacts observed between the pTyr and residues of the PLCC SH2 domain. In particular, residues Arg βB7, Ala βC3, His βD4, Cys βD5, and Arg βD6 make extensive contacts with the pTyr, with the majority of these NOEs involving the aromatic ring protons.

While there are explicit protein–peptide NOEs to only two of the four Args that potentially interact with the pTyr, the structures and other NMR evidence allow us to describe the interactions of all four residues. The NOEs and resulting structures show that Arg βD6 interacts strongly with the Tyr ring π electrons. The NOEs involving Arg βB7 may be indicative of interactions with the ring or the phosphate. While there are no protein–peptide NOEs to Arg βB5, the structures clearly locate this residue at the base of the pTyr-binding pocket. Slowly exchanging guanidinium Nε and Nη protons, with distinct ^{15}N and proton chemical shifts, indicate a pair of stable hydrogen bonds from two Nη protons to phosphate oxygens. There are also no protein–peptide NOEs involving Arg αA2. The structures allow for the possibility of guanidinium–phosphate hydrogen bonds and the large chemical shift change of 0.9 ppm for the CαH resonance upon addition of phosphopeptide is consistent with close contact of the pTyr to this residue. The results are consistent with the high conservation of these residues in SH2 domains (Koch et al., 1991) and with mutational analyses (Valius et al., 1993; Mayer et al., 1992; Marengere and Pawson, 1992; Bibbins et al., 1993) and crystallographic studies (Waksman et al., 1992, 1993; Eck et al., 1993) showing them to be important in pTyr binding.

Absence of direct NOEs between the pTyr and Arg βB5 and Arg αA2 residues can be explained by a number of factors. Formation of a stable hydrogen bond between Arg guanidinium groups and phosphate oxygens or the Tyr ring π electrons does not require that the distance between nonlabile NMR-observable protons be within 5 Å, since there are no stable protons on the phosphate of the pTyr. Distances between the potentially NMR-observable Cδ protons of Arg αA2 and Arg βB5 and the Cε ring protons of the pTyr in the Src structure vary from 6 to 7 Å, too far to detect NOEs. In addition, the side chain proton resonances of these four Args exhibit the severe broadening characteristic of intermediate exchange, reflecting dynamic processes on a millisecond timescale and resulting in a loss of signal intensity. Since each guanidinium group contains five nitrogen-bound protons, it may be that these potential hydrogen bond donor groups are exchanging positions as the complex samples various interactions, leading to resonance broadening. Preliminary ^{31}P NMR data do suggest the presence of multiple phosphorus environments, which are indicative of exchange. Other millisecond timescale motions may also contribute to the broadening. Another possible explanation is the low pH (6.4) of the sample. The second pK_A of free pTyr is in the range of 5.7–5.8 (Domchek et al., 1992). The extremely dense positive charge in the pTyr-binding pocket should lower the pK_A dramatically, giving two complete negative charges at pH 6.4, but it is possible that there is some exchange of the protonation state of the phosphate.

Hydrophobic Binding Groove

Residues C-terminal to the pTyr in the pY1021 peptide interact with a large hydrophobic cavity in the PLCC SH2 domain (see Figure 5B). This cavity begins at the βD strand and continues in an orthogonal direction to the strand. The groove is formed principally by the last residue of strand βE and residues of the EF and BG loops and primarily contacts peptide residues at the +1 and the +3 positions relative to the pTyr. The aromatic rings of Phe βC6 and Tyr BG3 and the aliphatic chain of Lys βD3 converge at one end of the channel (see Figure 5A) to form a binding pocket for the Ile at position +1 relative to the pTyr (Ile +1). NOEs were observed to all aliphatic proton resonances of Ile +1, and a hydrogen bond is present between the amide proton of Ile +1 and the carbonyl of His βD4. Note that the PLCC SH2 domain has the highest binding selectivity at the +1 position (a 3.7-fold preference for Ile; Songyang et al., 1993). Numerous NOEs were observed between Pro +3 and the Cδ methyl groups of Leu βE4 and Leu BG2 (Figure 6B), reflecting the deep binding of the Pro ring into the channel formed between the EF and BG loops and explaining the observed preference for Pro at the +3 position. The precision of atomic positions determined for this region of the interface seen in the superposition of heavy atoms presented in Figure 4 is due to the high density of NOEs for these residues.

A number of NOEs were found from residues of the SH2 domain to residues in the +4, +5, and +6 positions of the pY1021 peptide (Figure 6C). Leu +4 is situated in the cleft between the EF and BG loops. The peptide backbone changes direction beginning at Pro +5, following the path of the BG loop before extending into the solvent. This position may be stabilized by a salt bridge between Asp +6 and Arg BG4, Lys BG5, or His αB12. The electrostatic interactions may explain the binding preference of the PLCC SH2 domain for the PDGFR over the EGFR, since the residue in the +6 position in the high affinity binding site for PLCC SH2 in the EGFR is a Gly (Ullrich et al.,

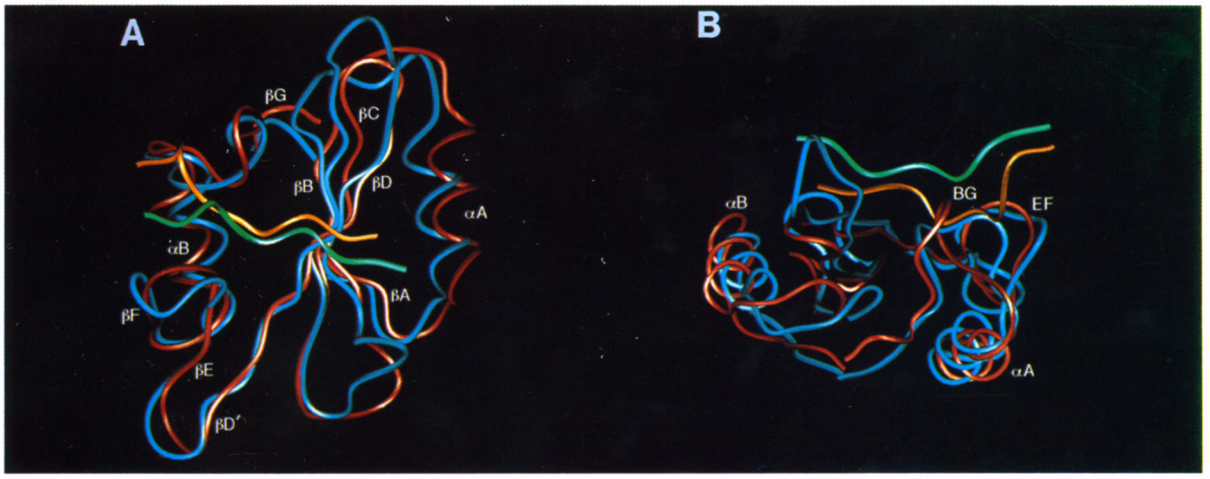

Figure 7. Superposition of a Ribbon Diagram Representation of the Src SH2–Phosphopeptide Complex with the PLCC–pY1021 Complex

The Src SH2 domain is shown in blue with its bound peptide in green, while the PLCC SH2 is colored red and the pY1021 peptide is orange.
(A) View facing the peptide binding surface, showing the overall similarity of the tertiary fold and position of the phosphopeptide.
(B) View looking perpendicular to the peptide binding surface, showing the relative position of the phosphopeptides in the binding site. Note that the PLCC SH2-binding phosphopeptide (in orange) binds more deeply into the SH2 domain than does the Src SH2-binding peptide.

1984). Among the sites known to or speculated to bind with high affinity to the PLCC SH2 domain (Songyang et al., 1993), only the PDGFR α (Claesson-Welsh et al., 1989) and β contain an acidic residue at the +6 position, although the FGFR family contains an Asp residue at the +4 position. Overall, the sequences of these PLCC SH2-binding sites, including the EGFR Tyr-992 (Ullrich et al., 1984), Let-23 Tyr-1244 (Aroian et al., 1990), Flg Tyr-558, Bek Tyr-551, FGFR-4 Tyr-547 (Partanen et al., 1991), and human Erb-B2 Tyr-1127 (Semba et al., 1985) sites, are divergent beyond the +3 position.

Approximately 85% of protein–peptide NOE peaks involve pTyr, Ile +1, or Pro +3. Only one unambiguously assigned NOE was found to involve Ile +2. In the structures, the EF loop contacts the Cγ methyl of Ile +2, while the Cγ methylene and Cδ methyl of this residue face the solvent. These results are consistent with the binding preferences of the PLCC SH2 domain for hydrophobic amino acids at the +2 position (Songyang et al., 1993), but do not provide a convincing explanation for the 2-fold strength of this preference. A higher resolution structure of this complex (refinement in progress) may shed light on this issue.

Discussion

Comparison with Src/Lck SH2 Complexes

Our comparison of the details of binding of this pY1021 peptide to the PLCC SH2 with the binding of the pTyr–Glu–Glu–Ile peptide to the Src (Waksman et al., 1993) and Lck (Eck et al., 1993) SH2 domains will focus on the Src complex since the SH2–peptide interactions are nearly identical in the Src and Lck structures. The backbone folds of the SH2 domains are very similar (Figure 7), with a backbone RMSD between the Src and the minimized average PLCC SH2 domains of 1.1 Å. The most pronounced conformational differences occur in the loops, particularly the BC and BG loops, as well as in the side chains that interact with the peptide. When viewed face on to the peptide binding surface (Figure 7A), the position of the peptide is very similar in Src and PLCC; both lie predominantly orthogonal to the central β sheet, although the PLCC-bound peptide curves at its C-terminus to follow the BG loop. A view perpendicular to the peptide binding surface (Figure 7B) shows that the PLCC-bound peptide penetrates considerably deeper into the binding groove and interacts much more extensively with the SH2 domain than does the Src-bound peptide.

The presence of four Arg residues at positions αA2, βB5, βB7, and βD6 that could potentially interact with the pTyr is unique to the PLCC SH2 domain. Arg βB5 is positioned at the base of the binding pocket and contributes two Nη protons to hydrogen bonds with the pTyr phosphate group in both the Src and PLCC complexes. The backbone of Arg αA2 is positioned similarly relative to the pTyr in each complex, and the guanidinium group forms two Hη-aromatic hydrogen bonds and one Hε-phosphate hydrogen bond in the Src complex. NMR structures and chemical shift arguments place the backbone of Arg αA2 near the pTyr phosphate group in the PLCC complex; however, interaction with the guanidinium group is less certain. The Src SH2 domain has a Ser at the βB7 position that hydrogen bonds to the pTyr phosphate group via its hydroxyl group. Arg βB7 in the PLCC SH2 domain also may hydrogen bond to the phosphate group and may be able to form additional hydrogen bonds to the ring owing to its increased length and increased number of donors. Arg βD6 is replaced by a Lys in Src, but each of these residues interacts strongly with the pTyr ring, forming amino–aromatic hydrogen bonds in the case of Src and probably

also in PLCC. The principle difference in the pTyr-binding region may be the additional potential hydrogen bond–donating groups in the PLCC SH2 domain. While Arg βB5 at the base of the pTyr-binding site is involved in stable hydrogen bonds, each of the three other Arg guanidinium groups may compete for and exchange hydrogen bonds, resulting in a more dynamic interaction than in the Src complex.

In the crystal structures of Src–phosphopeptide complexes, phosphate binding involves the formation of an extensive hydrogen bonding network from residues Glu BC1 and Thr BC2 in the BC loop of the SH2 domain to the phosphate of the pTyr. However, NOEs between the pTyr of the pY1021 peptide and residues in the BC loop of the PLCC SH2 domain were not observed. Significant changes in chemical shifts and backbone dynamics were also not observed in the BC loop upon addition of the pY1021 peptide (Farrow et al., 1994). Although the amide–water exchange rate of Asn BC1 decreases significantly upon binding of the pY1021 peptide, it is unlikely that the BC loop in the PLCC SH2 domain is intimately involved in pTyr binding. This difference may be traced to specific amino acid substitutions. The side chain hydroxyl of Src Thr BC2 forms a hydrogen bond to the phosphate group. The equivalent residue in the PLCC SH2 domain is a Glu that would be repelled by the negatively charged phosphate group. The hydroxyl of the following residue in Src, Thr BC3, interacts indirectly by hydrogen bonding to and positioning the amino group of Lys βD6 over the pTyr ring. The BC3 position is deleted in the PLCC SH2 domain. Furthermore, the closest equivalent residue is Pro BC4, which cannot mimic this interaction. The interactions lost from this so-called phosphate-binding loop may be compensated by interactions from other residues, such as additional potential hydrogen bonding interactions with Args substituted for Lys βD6 and Ser βB7 in the Src and Lck SH2 domains. In this regard it is interesting to mention that the mutation of Ser βB7 in Abl eliminates pTyr binding (Mayer et al., 1992), but that the N-terminal SH2 domain of the p85α subunit of PI3K has an Ala at this position and Sem-5 has a Cys. Note that the Vav SH2 is similar to PLCC, with an Arg at βB7. In addition, certain of the phosphatase SH2 domains lack the Arg αA2, and mutation of the GTPase-activating protein N-terminal SH2 Arg αA2 to Ala, while reducing the affinity, did not abolish pTyr binding (Marengere and Pawson, 1992).

The binding of peptide residues C-terminal to the pTyr exhibit the most pronounced difference from the analogous Src- and Lck-binding sites. Src and other SH2 domains that bind peptides containing pTyr–hydrophilic–hydrophilic–Ile/Pro sequences have a bulky aromatic ring at position βD5, either Tyr (as in Src) or Phe. This position is substituted by a smaller Cys or Ile in PLCC and other SH2 domains that bind peptides containing pTyr–hydrophobic–X–hydrophobic sequences (Songyang et al., 1993). This results in a significant volume change, creating additional space for a larger pocket, and allows Phe βC6 to interact strongly with the the peptide, forming the base of the binding site for the +1 position. Val βC6 is inaccessible to the peptide in the Src complex. In addition, a salt bridge is formed between Arg EF3 and Asp BG2 in the Src SH2 domain, effectively joining the BG and EF loops and limiting the extent of the cavity and possible interactions with residues C-terminal to the +3 position. A comparable salt bridge does not occur in the PLCC SH2 domain, allowing interactions with the peptide at positions +4, +5, and +6.

Another difference between the PLCC SH2–pY1021 complex and the Src SH2–peptide complex is the role of the BG loop. In the Src SH2 domain, the BG loop contacts only the +3 residue, while in the PLCC SH2, the BG loop interacts with pY1021 peptide residues at the +1, +3, +4, +5, and +6 positions. We have observed a different conformation of the BG loop to that seen in the Src SH2 domain, undoubtedly related to these more extensive interactions.

Implications for Other SH2-Mediated Protein Interactions

Binding studies of random peptide libraries have focused the region of SH2 binding specificity to three residues C-terminal of pTyr (Songyang et al., 1993). This is consistent with the Src and Lck SH2 complexes with the pTyr–Glu–Glu–Ile peptide in which protein binding was not observed beyond the +3 position. However, in a recent study, a requirement for a Leu residue at the +4 position for specific binding of PLC-γ1 to the PDGFR was noted (Larose et al., 1993). Other binding studies with the Src (Bibbins et al., 1993) and Nck (Nishimura et al., 1993) SH2 domains indicate a requirement for residues N-terminal to the pTyr residue for optimal binding. From our structural results, there is clear evidence of SH2 binding of the pY1021 peptide extending from the pTyr to the +6 residue. The degree to which interactions with the +4, +5, and +6 residues contribute to high affinity-specific binding is not yet clear. Particular SH2–peptide complexes may reveal different requirements for residues outside the pTyr to +3 binding positions. Thus, it is important to extend peptide binding studies of SH2 domain specificity to include amino acids in positions +4, +5, and +6, as well as residues N-terminal to pTyr.

As our results for the PLCC–pY1021 complex demonstrate, the mode of pTyr binding can vary in different SH2–phosphopeptide complexes. This binding is dependent on hydrogen bonds and charge–charge interactions between the SH2 domain and pTyr. The fact that SH2 domains have sequence variations at positions implicated in pTyr binding suggests that there are a number of possibilities for these interactions and that a given SH2 domain will bind to a phosphopeptide using a selected subset of these interactions. There is also a dynamic component allowing a given SH2 domain to sample multiple interactions while bound to its target site, which is possible in the case of the PLCC–pY1021 complex.

The sequence-specific binding of SH2 domains to residues C-terminal to the pTyr similarly requires many electrostatic and van der Waals interactions. The structure of the PLCC SH2 domain complexed with the pY1021 peptide provides a model for interaction of SH2 domains with

sequences containing the pTyr–hydrophobic–X–hydrophobic motif. The openness of the binding groove for positions +1 to +6 also suggests other potential backbone conformations and interactions for different SH2–phosphopeptide complexes. These conformations could include those that curve toward the EF loop rather than the BG loop or those that do not curve and interact instead with residues of αB. The diversity of SH2 sequences and the possibility of multiple modes of SH2–phosphopeptide binding is not surprising given the many different protein interactions in signaling that these complexes mediate.

Experimental Procedures

Expression and Purification of the PLCC SH2 Domain

PLCC (Stahl et al., 1988), comprising residues 663–759 of the full enzyme, was subcloned into the pET-11d plasmid (Studier et al., 1990) and transformed into E. coli BL21 cells. In addition, the recombinant construct contains five additional residues N-terminal and three additional residues C-terminal to sequences of the PLCC SH2 domain in the intact PLC-γ1. Isotopically enriched SH2 domain (99% ^{13}C and ^{15}N labeled) was prepared by growth and induction of 2 liters of bacterial culture in M9 medium containing 1 g/l $^{15}NH_4Cl$ and 3 g/l ^{13}C-glucose. After induction with 1 mM IPTG, cells were harvested and lysed by sonication, and the overexpressed protein was purified to homogeneity by use of phosphocellulose, phenyl–Sepharose, and FPLC Mono S column chromatography. Purity was estimated at 99% by SDS–PAGE analysis. N-terminal amino acid sequencing and amino acid analysis confirmed the identity of the purified SH2 domain. Because of the presence of a Cys residue in the SH2 domain sequence, NMR samples were reduced with over 100-fold excess DTT, followed by dialysis in argon-purged buffers. NMR tubes were argon purged prior to addition of sample, sealed, and blanketed with argon for at least 10 min. The pY1021 peptide, a 12 residue phosphopeptide derived from the sequence surrounding Tyr-1021 of the PDGFR (DNDpYIIPLPDPK), was synthesized as described previously (Piccione et al., 1993).

NMR Techniques

NMR experiments were performed on Varian UNITY 500 MHz spectrometers equipped with pulsed-field gradient units and triple resonance probes with actively shielded z gradients. NMR spectra were processed using commercially available and in-house routines, as well as the NMRPipe software system (Delaglio, 1993), and analyzed using the programs PIPP and CAPP (Garrett et al., 1991) on SUN Sparc stations. Spectra recorded for sequential assignment and determination of protein–protein NOEs include 150 ms mixing time 3D ^{13}C- and ^{15}N-edited NOESY–HSQC (Marion et al., 1989; Ikura et al., 1990), 45 ms mixing time 3D ^{15}N-edited TOCSY–HSQC (Marion et al., 1989; Bax et al., 1990), 150 ms and 50 ms mixing time CN NOESY–HSQC (Pascal et al., 1994), and the (Hβ)CβCα(CO)NNH (Grzesiek and Bax, 1992) and HNCαCβ (Wittekind and Müeller, 1993) triple resonance experiments. Side chain assignments were obtained from HCCH–TOCSY (Kay et al., 1993) spectra and from experiments that correlate the aliphatic side chain ^1H and ^{13}C chemical shifts with the subsequent ^{15}N and NH shifts (Grzesiek et al., 1992; Montelione et al., 1992; Logan et al., 1992). (Hβ)Cβ(CγCδ)Hδ and (Hβ)Cβ(CγCδCε)Hε experiments were used for assignment of aromatic resonances (Yamazaki et al., 1993). All experiments incorporated pulsed-field gradients to suppress artifacts and assist in the elimination of the water resonance. Experiments involving observation of the NH proton made use of the enhanced sensitivity approach described previously (Kay et al., 1992; Muhandiram and Kay, 1994). The HMQC J experiment (Kay and Bax, 1990) was used to determine the three-bond NH–CαH coupling constants ($^3J_{HN\alpha}$) that were measured by fitting the line shape of one-dimensional traces through the HMQC J spectrum (Forman-Kay et al., 1990). Qualitative amide exchange rates were also measured from a cross section of the ^{15}N-edited NOESY–HSQC at the F_1 chemical shift of the water. Since this experiment was performed using gradients rather than presaturation to suppress water, amide–water exchange cross peaks can be observed at the F_1 chemical shift of water and their intensities can be qualitatively correlated with the rate of exchange. Double-filtered 2D proton NMR experiments for assignment of resonances of the pY1021 peptide include F_1,F_2 $^{13}C/^{15}N$-filtered NOESY, TOCSY, and COSY. A sample that contained a 1:2 protein:peptide ratio was also used to allow observation of exchange peaks between the resonances of the free and complexed pY1021 peptide. This information was utilized together with assignments of the free pY1021 peptide (i.e., in the absence of the SH2 domain) derived from homonuclear TOCSY experiments to assist assignment of the bound peptide. Over 98% of NMR-observable resonances of the SH2 domain and pY1021 peptide were unambiguously assigned. The primary exceptions are resonances of the two N-terminal residues Gly-1 and Ser-2 that are not a part of the PLC-γ1 SH2 domain sequence but are derived from the recombinant construct. 2D F_1,F_2 $^{13}C/^{15}N$-filtered NOESY experiments were used to extract peptide–peptide NOE peaks. A 3D F_1-edited, F_3-filtered ^{13}C-HMQC–NOESY was used to obtain protein–peptide NOE correlations.

Structure Calculations

Combined distance geometry-simulated annealing calculations were performed in a similar manner to those described previously (Nilges et al., 1988) using the program X-PLOR (Brünger, 1992). Calculations included 1104 protein–protein NOE-derived restraints and 65 ϕ and 7 ψ torsion angle restraints derived from $^3J_{HN\alpha}$ coupling constants and short mixing time intraresidue and sequential NOE values. The program STEREOSEARCH (Nilges et al., 1990) was utilized to extract the values for these torsion angle restraints. Stereospecific assignments of β-methylene protons and χ torsion angle restraints were not determined, in general, with the exception of χ^1 values for eight residues of the SH2 domain and two of pY1021 peptide. Center averaging of distances involving methylene, methyl, and ring protons was used, with appropriate corrections made to the values. The calculation also included 50 hydrogen-bonding restraints, based on qualitative amide–water exchange rates and NOEs defining the acceptor for 25 hydrogen bonds. A total of 98 NOE distance restraints between the PLCC SH2 domain and pY1021 peptide and 37 restraints within the pY1021 were also included. The mean structure generated by averaging the coordinates of the least-squares best-fitted structures was minimized, restraining the coordinates with the experimental NMR data as in the final steps of the simulated annealing calculations. This minimized structure satisfies the restraints from the experimental NMR data and covalent geometry as well as the individual structures and is used in Figures 5 and 7. Simulated annealing and minimization calculations included repulsive van der Waals terms only, with no full Lennard–Jones potential. Electrostatic terms were also not included.

Acknowledgments

We thank Ouwen Zhang for his measurements of the $^3J_{HN\alpha}$ coupling constants, Dr. Ranjith Muhandiram for assistance in recording some of the spectra, and Dr. John Kuriyan for use of the coordinates of the Src–pYEEI complex. S. M. P. is supported by a fellowship from the Medical Research Council of Canada (MRC). This research was supported by grants from the National Cancer Institute of Canada (NCIC) to J. D. F.-K. and L. E. K., with funds from the National Cancer Society, and from the MRC to T. P. T. P. is a Terry Fox Cancer Research Scientist of the NCIC.

Received March 23, 1994; revised April 5, 1994.

References

Anderson, D., Koch, C. A., Grey, L., Ellis, C., Moran, M. F., and Pawson, T. (1990). Binding of SH2 domains of phospholipase Cγ1, GAP, and Src to activated growth factor receptors. Science *250*, 979–982.

Aroian, R. V., Koga, M., Mendel, J. E., Ohshima, Y., and Sternberg, P. W. (1990). The *let-23* gene necessary for *Caenorhabditis elegans* vulval induction encodes a tyrosine kinase of the EGF receptor subfamily. Nature *348*, 693–699.

Bax, A., Clore, G. M., and Gronenborn, A. M. (1990). ^1H-^1H correlation via isotropic mixing of ^{13}C magnetization: a new three-dimensional

approach for assigning ^{1}H and ^{13}C spectra of ^{13}C-enriched proteins. J. Magn. Reson. *88*, 425–431.

Bibbins, K. B., Boeuf, H., and Varmus, H. E. (1993). Binding of the Src SH2 domain to phosphopeptides is determined by residues in both the SH2 domain and the phosphopeptides. Mol. Cell. Biol. *13*, 7278–7287.

Booker, G. W., Breeze, A. L., Downing, A. K., Panayotou, G., Gout, I., Waterfield, M. D., and Campbell, I. D. (1992). Structure of an SH2 domain of the p85α subunit of phosphatidylinositol-3-OH kinase. Nature *358*, 684–687.

Brünger, A. T. (1992). X-PLOR Version 3.1: A System for X-Ray Crystallography and NMR (New Haven, Connecticut: Yale University Press).

Cantley, L. C., Auger, K. R., Carpenter, C., Duckworth, B., Graziani, A., Kapeller, R., and Soltoff, S. (1991). Oncogenes and signal transduction. Cell *64*, 281–302.

Claesson-Welsh, L., Eriksson, A., Westermark, B., and Heldin, C.-H. (1989). cDNA cloning and expression of the human A-type platelet-derived growth factor (PDGF) receptor establishes structural similarity to the B-type PDGF receptor. Proc. Natl. Acad. Sci. USA *86*, 4917–4921.

Delaglio, F. (1993). NMRPipe System of Software (Bethesda, Maryland: National Institutes of Health).

Domchek, S. M., Auger, K. R., Chatterjee, S., Burke, T. R., and Shoelson, S. E (1992). Inhibition of SH2 domain/phosphoprotein association by a nonhydrolyzable phosphononopeptide. Biochemistry *31*, 9865–9870.

Eck, M. J., Shoelson, S. E., and Harrison, S. C. (1993). Recognition of a high-affinity phosphotyrosyl peptide by the Src homology-2 domain of $p56^{lck}$. Nature *362*, 87–91.

Farrow, N. A., Muhandiram, R., Singer, A. U., Pascal, S. M., Kay, C. M., Shoelson, S. E., Pawson, T., Forman-Kay, J. D., and Kay, L. E. (1994). Backbone dynamics of a free and phosphopeptide-complexed Src homology 2 domain studied by ^{15}N NMR relaxation. Biochemistry, in press.

Forman-Kay, J. D., Gronenborn, A. M., Wingfield, P., and Clore, G. M. (1990). Studies on the solution conformation of human thioredoxin using heteronuclear ^{15}N-^{1}H nuclear magnetic resonance spectroscopy. Biochemistry *29*, 1566–1572.

Garrett, D. S., Powers, R., Gronenborn, A. M., and Clore, G. M. (1991). A common sense approach to peak picking in two-, three-, and four-dimensional spectra using automatic computer analysis of contour diagrams. J. Magn. Reson. *95*, 214–220.

Grzesiek, S., and Bax, A. (1992). Correlating backbone amide and side chain resonances in larger proteins by multiple relayed triple resonance NMR. J. Am. Chem. Soc. *114*, 6291–6293.

Grzesiek, S., Anglister, J., and Bax, A. (1992). Correlation of backbone amide and aliphatic side-chain resonances in ^{13}C/^{15}N enriched proteins by isotropic mixing of ^{13}C magnetization. J. Magn. Reson. (B) *101*, 114–119.

Ikura, M., and Bax, A. (1992). Isotope-filtered 2D NMR of a protein–peptide complex: study of a skeletal muscle myosin light chain kinase fragment bound to calmodulin. J. Am. Chem. Soc. *114*, 2433–2440.

Ikura, M., Kay, L. E., Tschudin, R., and Bax, A. (1990). Three-dimensional NOESY–HMQC spectroscopy of a ^{13}C-labeled protein. J. Magn. Reson. *86*, 204–209.

Kay, L. E., and Bax, A. (1990). New methods for the measurement of NH–CαH coupling constants in ^{15}N-labeled proteins. J. Magn. Reson. *86*, 110–126.

Kay, L. E., Keifer, P., and Saarinen, T. (1992). Pure absorption gradient enhanced heteronuclear single quantum correlation spectroscopy with improved sensitivity. J. Am. Chem. Soc. *114*, 10663–10665.

Kay, L. E., Xu, G.-Y., Singer, A. U., Muhandiram, D. R., and Forman-Kay, J. D. (1993). A gradient enhanced HCCH–TOCSY experiment for recording side-chain ^{1}H and ^{13}C correlations in H_2O samples of proteins. J. Magn. Reson. (B) *101*, 333–337.

Koch, C. A., Anderson, D., Moran, M. F., Ellis, C., and Pawson, T. (1991). SH2 and SH3 domains: elements that control interactions of cytoplasmic signaling proteins. Science *252*, 668–674.

Larose, L., Gish, G., Shoelson, S., and Pawson, T. (1993). Identification of residues in the β platelet-derived growth factor receptor that confer specificity for binding to phospholipase C-γ1. Oncogene *8*, 2493–2499.

Logan, T. M., Olejniczak, E. T., Xu, E. T., and Fesik, S. W. (1992). Side chain and backbone assignments in isotopically labeled proteins from two heteronuclear triple resonance experiments. FEBS Lett. *314*, 413–418.

Marengere, L. E. M., and Pawson, T. (1992). Identification of residues in GTPase-activating protein Src homology 2 domains that control binding to tyrosine phosphorylated growth factor receptors and p62. J. Biol. Chem. *267*, 22779–22786.

Marion, D., Driscoll, P. C., Kay, L. E., Wingfield, P. T., Bax, A., Gronenborn, A. M., and Clore, G. M. (1989). Overcoming the overlap problem in the assignment of ^{1}H NMR spectra of larger proteins by use of three-dimensional heteronuclear ^{1}H-^{15}N Hartmann–Hahn-multiple quantum coherence and nuclear Overhauser-multiple quantum coherence spectroscopy: application to interleukin 1β. Biochemistry *28*, 6150–6156.

Mayer, B. J., Jackson, P. K., Van Etten, R. A., and Baltimore, D. (1992). Point mutations in the *abl* SH2 domain coordinately impair phosphotyrosine binding *in vitro* and *in vivo*. Mol. Cell. Biol. *12*, 609–618.

Mohammadi, M., Honegger, A. M., Rotin, D., Fischer, R., Bellot, F., Li, W., Dionne, C. A., Jaye, M., Rubinstein, M., and Schlessinger, J. (1991). A tyrosine-phosphorylated carboxy-terminal peptide of the fibroblast growth factor receptor (Flg) is a binding site for the SH2 domain of phospholipase C-γ1. Mol. Cell. Biol. *11*, 5068–5078.

Mohammadi, M., Dionne, C. A., Li, W., Li, N., Spivak, T., Honegger, A. M., Jaye, M., and Schlessinger, J. (1992). Point mutation in FGF receptor eliminates phosphatidylinositol hydrolysis without affecting mitogenesis. Nature *358*, 681–684.

Montelione, G. T., Lyons, B. A., Emerson, S. D., and Jashiro, M. (1992). An efficient triple resonance experiment using carbon-13 isotropic mixing for determining sequence-specific resonance assignments of isotopically-enriched proteins. J. Am. Chem. Soc. *114*, 10974–10975.

Moran, M. F., Koch, C. A., Anderson, D., Ellis, C., England, L., Martin, G. S., and Pawson, T. (1990). Src homology region 2 domains direct protein–protein interactions in signal transduction. Proc. Natl. Acad. Sci. USA *87*, 8622–8626.

Muhandiram, D. R., and Kay, L. E. (1994). Gradient enhanced triple resonance three dimensional NMR experiments with improved sensitivity. J. Magn. Reson. (B) *103*, 203–216.

Nicholls, A., Sharp, K. A., and Honig, B. (1991). Protein folding and association: insights from the interfacial and thermodynamic properties of hydrocarbons. Protein Struct. Funct. Genet. *11*, 281–296.

Nilges, M., Clore, G. M., and Gronenborn, A. M. (1988). Determination of three-dimensional structures of proteins from interproton distance data by hybrid distance geometry-dynamical simulated annealing calculations. FEBS Lett. *239*, 317–324.

Nilges, M., Clore, G. M., and Gronenborn, A. M. (1990). ^{1}H-NMR stereospecific assignments by conformational data-base searches. Biopolymers *29*, 813–822.

Nishimura, R., Li, W., Kashishian, A., Mondino, A., Zhou, M., Cooper, J., and Schlessinger, J. (1993). Two signaling molecules share a phosphotyrosine-containing binding site in the platelet-derived growth factor receptor. Mol. Cell. Biol. *13*, 6889–6896.

Overduin, M., Mayer, B., Rios, C. B., Baltimore, D., and Cowburn, D. (1992a). Secondary structure of Src homology 2 domain of c-*abl* by heteronuclear NMR spectroscopy in solution. Proc. Natl. Acad. Sci. USA *89*, 11673–11677.

Overduin, M., Rios, C. B., Mayer, B. J., Baltimore, D., and Cowburn, D. (1992b). Three-dimensional solution structure of the Src homology 2 domain of c-*abl*. Cell *70*, 697–704.

Partanen, J., Makela, T. P., Eerola, E., Korhonen, J., Hirvonen, H., Claesson-Welsh, L., and Alitalo, K. (1991). FGF-4, a novel acidic fibroblast growth factor receptor with a distinct expression pattern. EMBO J. *10*, 1347–1354.

Pascal, S., Muhandiram, D. R., Yamazaki, T., Forman-Kay, J. D., and Kay, L. E. (1994). Simulataneous acquisition of ^{15}N and ^{13}C edited NOE

spectra of proteins dissolved in H_2O. J. Magn. Reson. (B) *101*, 197–201.

Pawson, T., and Gish, G. D. (1992). SH2 and SH3 domains: from structure to function. Cell *71*, 359–362.

Pawson, T., and Schlessinger, J. (1993). SH2 and SH3 Domains. Curr. Biol. *3*, 434–442.

Pawson, T., Olivier, P., Rozakis-Adcock, M., McGlade, J., and Henkemeyer, M. (1993). Proteins with SH2 and SH3 domains couple receptor tyrosine kinases to intracellular signaling pathways. Phil. Trans. Roy. Soc. (Lond.) B *340*, 279–285.

Peters, K. G., Marie, J., Wilson, E., Ives, H. E., Escobedo, J., Del Rosario, M., Mirda, D., and Williams, L. T. (1992). Point mutation of an FGF receptor abolishes phosphtidylinositol turnover and Ca^{2+} flux but not mitogenesis. Nature *358*, 678–681.

Piccione, E., Case, R. D., Domchek, S. M., Hu, P., Chaudhuri, M., Backer, J. M., Schlessinger, J., and Shoelson, S. E. (1993). Phosphatidylinositol 3-kinase p85 SH2 domain specificity defined by direct phosphopeptide/SH2 domain binding. Biochemistry *32*, 3197–3202.

Rhee, S. G. (1991). Inositol phospholipid-specific phospholipase C: interaction of the γ_1 isoform with tyrosine kinase. Trends Biochem. Sci. *16*, 297–301.

Rotin, D., Margolis, B., Mohammadi, M., Daly, R. J., Daum, G., Li, N., Fischer, E. H., Burgess, W. H., Ullrich, A., and Schlessinger, J. (1992). SH2 domains prevent tyrosine dephosphorylation of the EGF receptor: identification of Tyr992 as the high-affinity binding site for SH2 domains of phospholipase C-γ. EMBO J. *11*, 559–567.

Semba, K., Kamata, N., Toyoshima, K., and Yamamato, T. (1985). A v-*erβB*-related protooncogene, c-*erβB-2*, is distinct from the c-*erβB-1*/epidermal growth-factor-receptor gene and is amplified in a human salivary gland adenocarcinoma. Proc. Natl. Acad. Sci. USA *82*, 6497–6501.

Songyang, Z., Shoelson, S. E., Chaudhuri, M., Gish, G., Pawson, T., Haser, W. G., King, F., Roberts, T., Ratnofsky, S., Lechleider, R. J., Neel, B. G., Birge, R. B., Fajardo, J. E., Chou, M. M., Hanafusa, H., Schaffhausen, B., and Cantley, L. C. (1993). SH2 domains recognize specific phosphopeptide sequences. Cell *72*, 767–778.

Songyang, Z., Shoelson, S. E., McGalde, J., Olivier, P., Pawson, T., Bostelo, R. X., Barbacid, M., Sabe, H., Hanafusa, H., Yi, T., Reu, R., Baltimore, D., Ramofsky, S., Feldman, R. A., and Cantley, C. (1994). Specific motifs recognized by the SH2 domains of csk, 3BP2, fes/fps, Grb-2, SHPTP1, SHC, Syk and vav. Mol. Cell. Biol. *14*, 2777–2785.

Stahl, M. L., Ferenz, C. R., Kelleher, K. L., Kriz, R. W., and Knopf, J. L. (1988). Sequence similarity of phospholipase C with the non-catalytic region of src. Nature *332*, 269–272.

Studier, F. W., Rosenberg, A. H., Dunn, J. J., and Dubendorff, J. W. (1990). Use of T7 RNA polymerase to direct expression of cloned genes. Meth. Enzymol. *185*, 60–89.

Ullrich, A., Coussens, L., Hayflick, J. S., Dull, T. J., Gray, A., Tam, A. W., Lee, J., Yarden, Y., Libermann, T. A., Schlessinger, J., Downward, J., Mayes, E. L. V., Whittle, N., Waterfield, M. D., and Seeburg, P. H. (1984). Human epidermal growth factor receptor cDNA sequence and aberrant expression of the amplified gene in A431 epidermal carcinoma cells. Nature *309*, 418–425.

Valius, M., and Kazlauskas, A. (1993). Phospholipase C-γ1 and phosphatidylinositol 3 kinase are the downstream mediators of the PDGF receptor's mitogenic signal. Cell *73*, 321–334.

Valius, M., Bazenet, C., and Kazlauskas, A. (1993). Tyrosines 1021 and 1009 are phosphorylation sites in the carboxy terminus of the platelet-derived growth factor receptor β subunit and are required for binding of phospholipase Cγ and a 64-kilodalton protein, respectively. Mol. Cell. Biol. *13*, 133–143.

Waksman, G., Kominos, D., Robertson, S. C., Pant, N., Baltimore, D., Birge, R. B., Cowburn, D., Hanafusa, H., Mayer, B. J., Overduin, M., Resh, M. D., Rios, C. B., Silverman, L., and Kuriyan, J. (1992). Crystal structure of the phosphotyrosine recognition domain SH2 of v-*src* complexed with tyrosine phosphorylated peptides. Nature *358*, 646–653.

Waksman, G., Shoelson, S. E., Pant, N., Cowburn, D., and Kuriyan, J. (1993). Binding of a high affinity phosphotyrosyl peptide to the Src SH2 domain: crystal structures of the complexed and peptide-free forms. Cell *72*, 779–790.

Wittekind, M., and Müeller, L. (1993). HNCACB: a high sensitivity 3D NMR experiment to correlate amide proton and nitrogen resonances with the alpha- and beta-carbon resonances in proteins. J. Magn. Reson. (B) *101*, 201–205.

Yamazaki, T., Forman-Kay, J. D., and Kay, L. E. (1993). Two-dimensional NMR experiments for correlating $^{13}C_\beta$ and $^1H_{\delta/\epsilon}$ chemical shifts of aromatic residues in ^{13}C labeled proteins via scalar couplings. J. Am. Chem. Soc. *115*, 11054–11055.

Zhu, G., Decker, S. J., and Saltiel, A. R. (1992). Direct analysis of the binding of Src-homology 2 domains of phospholipase C to the activated epidermal growth factor receptor. Proc. Natl. Acad. Sci. USA *89*, 9559–9563.

Note Added in Proof

It has come to our attention that J. Kuriyan and colleagues have recently solved crystal structures of peptide complexes of a Syp pTyr SH2 domain, providing additional examples of SH2 interactions with peptides containing the pTyr–hydrophobic–X–hydrophobic motif. This information appears in the following article: Lee, C.-H., Kominos, D., Jacques, S., Margolis, B., Schlessinger, J., Shoelson, S. E., and Kuriyan, J. (1994). Crystal structures of peptide complexes of the N-terminal SH2 domain of the Syp tyrosine phosphatase. Structure, in press.